Towards understanding $b\bar{b}$ production in $\gamma\gamma$ collisions

Jiří Chýla*

Center for Particle Physics, Institute of Physics, Academy of Sciences of the Czech Republic, Na Slovance 2, 18221 Prague 8, Czech Republic

(Received 30 December 2003; revised manuscript received 2 June 2004; published 1 September 2004)

The data on the total cross section $\sigma_{\rm tot}(e^+e^- \to e^+e^- b\bar{b})$ measured at LEP2 represent a serious challenge for perturbative QCD. In order to understand the origin of the excess of data over QCD calculations, we investigate the dependence of the four contributions to this cross section on $\gamma\gamma$ collision energy. As the reliability of the existing calculations of $\sigma_{\rm tot}(e^+e^- \to e^+e^- b\bar{b})$ depends, among other things, on the stability of the calculations of the cross section $\sigma_{\rm tot}(\gamma\gamma \to b\bar{b})$ with respect to variations of the renormalization and factorization scales, we investigate this aspect in detail. We show that in most of the region relevant for the LEP2 data the existing QCD calculations of the cross section $\sigma_{\rm tot}(\gamma\gamma \to b\bar{b})$ do not exhibit a region of local stability. A possible source of this instability is suggested.

DOI: 10.1103/PhysRevD.70.054001 PACS numbers: 13.60.Hb, 11.25.Db, 12.38.Bx

I. INTRODUCTION

Heavy quark production in hard collisions of hadrons, leptons, and photons has been considered as a clean test of perturbative QCD. It has therefore come as a surprise that the first data on the $b\bar{b}$ production in $\bar{p}p$ collisions at the Tevatron [1,2], γp collisions at HERA [3,4], and $\gamma\gamma$ collisions at LEP2 [5,6] have turned out to lie significantly and systematically above theoretical calculations. The disagreement between data and theory [7–9] was particularly puzzling for the collisions of two quasireal photons at LEP2.

The arrival of new data on $b\bar{b}$ production in ep collisions at HERA have further complicated the situation. In the range of moderate $Q^2 \gtrsim 10$ GeV^2, the new ZEUS data [10] are in reasonable agreement with next-to-leading order (NLO) QCD predictions, but there is still a sizable excess of the new ZEUS data over theory in the region $2 \lesssim Q^2 \lesssim 10$ GeV^2. Moreover, there is a problem of consistency between new ZEUS and older H1 data in the region $Q^2 \gtrsim 10$ GeV^2. For $\bar{p}p$ collisions, the progress on the theoretical side [11,12] has significantly reduced the discrepancy observed at the Tevatron.

On the other hand, the problem of understanding the $b\bar{b}$ production in $\gamma\gamma$ collisions remains unsolved. The recent DELPHI data [13] are in striking agreement with the older L3 and OPAL data and by a factor of about 3 above the standard NLO QCD calculations. There have, however, been few theoretical suggestions of how to explain this excess. Neither the use of unintegrated parton distribution functions [14] nor the production of supersymmetric particles [15], proposed for explaining an analogous excess in antiproton-proton collisions, are of much help for LEP2 data, primarily because of low $\gamma\gamma$ energies involved.

*Email address: chyla@fzu.cz

In [12], we have investigated the sensitivity of QCD calculations of $\sigma_{\rm tot}(p\bar{p} \to b\bar{b})$ to variation of the renormalization and factorization scales μ and M. In particular, we have argued that in order to arrive at locally stable results [16] these two scales must be kept independent. We have furthermore shown that in the Tevatron energy range the position of the saddle point of the cross section $\sigma_{\rm tot}^{\rm NLO}(p\bar{p} \to b\bar{b}; S, M, \mu)$, considered as a function of μ and M, lies far away from the "diagonal" $\mu = M$ used in all existing QCD calculations. Using the NLO prediction at the saddle point instead of the conventional choice $\mu = M = m_b$ enhances the theoretical prediction in the Tevatron energy range by a factor of about 2, which may help in explaining part of the excess of data over NLO QCD predictions.

In this paper similar analysis is performed for $\gamma\gamma$ collisions at center of mass system energies W relevant for LEP2 data. Although all three experiments at LEP2 have measured merely an integral over the cross section $\sigma(\gamma\gamma \to b\bar{b}, W)$ weighted by the product of photon fluxes inside the beam electrons and positrons, it is very important to understand the W dependence of the four individual contributions to it.

The paper is organized as follows. In the following section, the general form of the perturbative expansion of the total cross section $\sigma_{\rm tot}(\gamma\gamma \to b\bar{b}; W, M, \mu)$ is reviewed and the role of three different classes of direct and resolved photon contributions is discussed. In Sec. III, the W dependence of the four contributions to the cross section $\sigma_{\rm tot}(e^+e^- \to e^+e^- b\bar{b})$ is investigated at the LO of QCD. The main result of this paper, the numerical study of the sensitivity of standard NLO approximation to $\sigma_{\rm tot}^{\rm NLO}(\gamma\gamma \to b\bar{b})$ to the choice of renormalization and factorization scales, is presented in Sec. IV. The conclusions are drawn in Sec. V.

II. $Q\overline{Q}$ PRODUCTION IN $\gamma\gamma$ COLLISIONS

Throughout the paper, I will adopt the standard terminology and notation used in the theoretical description of hard $\gamma\gamma$ collisions as defined, for instance, in [17]. The reader is referred to this paper also for a discussion of salient features of QCD description of the photon, such as the inhomogeneous nature of the evolution equations for its parton distribution functions (PDF), etc. As all PDF used below are those of the (quasi)real photon, I will drop any specification of this fact.

In the calculations of [7–9], performed with fixed pole quark masses, the NLO QCD approximation to $\sigma_{\rm tot}(\gamma\gamma \to Q\overline{Q})$ is defined by taking into account the first two terms in the perturbation expansions of direct

$$\sigma_{\rm dir}(M) = \sigma^{(0)}_{\rm dir} + \sigma^{(1)}_{\rm dir}\alpha_s(\mu) + \sigma^{(2)}_{\rm dir}(M,\mu)\alpha_s^2(\mu) + \sigma^{(3)}_{\rm dir}(M,\mu)\alpha_s^3(\mu) + \cdots, \tag{1}$$

as well as single

$$\begin{aligned}\sigma_{\rm sr}(M) &= 2\int dx\, G(x,M)\sigma_{\gamma G}(x,M) + 4\int dx \sum_i q_i(x,M)\sigma_{\gamma q_i}(x,M)\\ &= \sigma^{(1)}_{\rm sr}(M)\alpha_s(\mu) + \sigma^{(2)}_{\rm sr}(M,\mu)\alpha_s^2(\mu) + \sigma^{(3)}_{\rm sr}(M,\mu)\alpha_s^3(\mu) + \cdots,\end{aligned} \tag{2}$$

and double resolved photon contributions,

$$\begin{aligned}\sigma_{\rm dr}(M) &= 4\int dx\, dy \sum_i q_i(x,M)\overline{q}_i(y,M)\sigma_{q\overline{q}}(xy,M) + \iint dx\, dy\, G(x,M)G(y,M)\sigma_{GG}(xy,M)\\ &\quad +2\iint dx\, dy \Sigma(x,M)G(y,M)\sigma_{qG}(xy,M)\\ &= \sigma^{(2)}_{\rm dr}(M)\alpha_s^2(\mu) + \sigma^{(3)}_{\rm dr}(M,\mu)\alpha_s^3(\mu) + \cdots.\end{aligned} \tag{3}$$

In the above expressions, we have taken into account identity of beam particles and equality $q(x,M) = \overline{q}(x,M)$. The partonic cross sections appearing in (2) and (3) can be expanded in powers of $\alpha_s(\mu)$ in the following way:

$$\sigma_{\gamma G}(x,M) = \alpha_s(\mu)\sigma^{(1)}_{\gamma G}(x) + \alpha_s^2(\mu)\sigma^{(2)}_{\gamma G}(x,M,\mu) + \cdots, \tag{4}$$

$$\sigma_{\gamma q_i}(x,M) = \alpha_s^2(\mu)\sigma^{(2)}_{\gamma q_i}(x,M) + \alpha_s^3(\mu)\sigma^{(3)}_{\gamma q_i}(x,M,\mu) + \cdots, \tag{5}$$

and

$$\sigma_{q\overline{q}}(xy,M) = \alpha_s^2(\mu)\sigma^{(2)}_{q\overline{q}}(xy) + \alpha_s^3(\mu)\sigma^{(3)}_{q\overline{q}}(xy,M,\mu) + \cdots, \tag{6}$$

$$\sigma_{GG}(xy,M) = \alpha_s^2(\mu)\sigma^{(2)}_{GG}(xy) + \alpha_s^3(\mu)\sigma^{(3)}_{GG}(xy,M,\mu) + \cdots, \tag{7}$$

$$\sigma_{qG}(xy,M) = \alpha_s^3(\mu)\sigma^{(3)}_{qG}(xy,M) + \cdots. \tag{8}$$

Starting at order $\alpha\alpha_s^2$, the direct photon contribution depends also on the factorization scale and therefore mixes with the single and double resolved photon ones. The first two terms in (1) are, however, unrelated to any terms in (2) or (3) and can therefore be considered separately.

Note that PDF as well as the short distance parton level cross sections depend on the factorization scale M, whereas the renormalization scale μ appears only if the latter are calculated as perturbative expansions in $\alpha_s(\mu)$. As emphasized a long time ago by Politzer [18], these scales reflect ambiguities in the treatment of quite different divergences (ultraviolet in the case of the renormalization scale μ and infrared in the case of the factorization scale M) and should thus be kept as independent free parameters of any finite order perturbative calculation. Note also that each of the three contributions, (1)–(3), depends on the factorization scale M and only their sum is independent of M.

The approximations employed in [7–9] include all terms that are currently known, so we cannot presently do better. On the other hand, we should be aware of its theoretical status [19]. Clear shortcoming concerns the case of the direct contribution (1) which is the sum of the purely QED contribution

$$\begin{aligned}\sigma^{(0)}_{\rm dir}(W) &= \sigma_0\left[\left(1+\frac{4m_b^2}{W^2}-\frac{8m_b^4}{W^4}\right)\ln\frac{1+\beta}{1-\beta} - \beta\left(1+\frac{4m_b^2}{W^2}\right)\right]\\ &= \sigma_0 c^{(0)}(m_b/W),\\ \sigma_0 &\equiv \frac{12\pi e_b^4\alpha^2}{W^2},\end{aligned} \tag{9}$$

where $\beta = \sqrt{1-4m_b^2/W^2}$ and the lowest order QCD correction given as $\sigma^{(1)}_{\rm dir}\alpha_s = \sigma_0\alpha_s(\mu)c^{(1)}(m_b/W)$ and calculated, for instance, in [20]

$$\begin{aligned}\sigma^{(01)}_{\rm dir} &\equiv \sigma^{(0)}_{\rm dir} + \sigma^{(1)}_{\rm dir}\alpha_s\\ &= \sigma_0[c^{(0)}(m_b/W) + \alpha_s(\mu)c^{(1)}(m_b/W)].\end{aligned} \tag{10}$$

As the sum (10) does not mix to this order with the other two contributions (2) and (3), it is manifestly of the leading order in QCD coupling α_s only and thus a monotonous function of the renormalization scale μ. Consequently, it cannot be associated to a well-defined renormalization scheme of α_s as such an association requires the presence of at least two consecutive nontrivial powers of α_s.

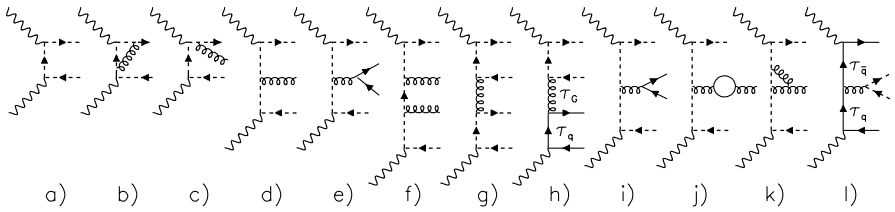

FIG. 1. Examples of diagrams describing the direct photon contribution to $\sigma(\gamma\gamma \to Q\overline{Q})$ up to the order $\alpha^2\alpha_s^2$. The solid (dashed) lines denote light (heavy) quarks.

At the order $\alpha^2\alpha_s^2$, the diagrams with light quarks appear, and we can distinguish three classes of direct photon contributions differing by the overall heavy quark charge factor CF:

Class A: $CF = e_Q^4$: Comes from diagrams, such as those in Figs. 1(e)–1(g), in which both photons couple to heavy $Q\overline{Q}$ pairs. Despite the presence of mass singularities in contributions of individual diagrams coming from gluons and light quarks in the final state and from loops, the Kinoshita-Lee-Naunberg theorem implies that at each order of α_s the sum of all contributions of this class to $\sigma_{\rm dir}$ is finite. As the first as well as the second terms in (10) are proportional to e_Q^4, it is this class of direct photon contributions that yields the third term in (10) and is thus needed for the calculation of $\sigma_{\rm dir}$ to be performed in a well-defined renormalization scheme (RS).

Class B: $CF = e_Q^2$: Comes from diagrams, such as that in Fig. 1(h), in which one of the photons couples to a heavy $Q\overline{Q}$ and the other to a light $q\overline{q}$ pair. For massless light quarks, this diagram has initial state mass singularity, which is removed by introducing the concept of the light quark distribution functions of the photon. The factorization scale dependence of the contribution of this diagram is then related to that of single resolved photon diagrams in Figs. 2(a) and 2(c).

Class C: $CF = 1$: Comes from diagrams in which both photons couple to light $q\overline{q}$ pairs, as those in Fig. 1(l). In this case, the analogous subtraction procedure relates it to the single resolved photon contribution of the diagram in Fig. 2(f) and double resolved photon contribution of the diagram in Fig. 2(h).

Because of different charge factors CF, the classes A, B, and C of direct photon contributions do not mix under renormalization of α_s and factorization of mass singularities.

Both the single and double resolved photon contribution, given by the first two terms in (2) and (3) contain two nonzero consecutive terms in expansion of partonic cross sections in α_s and thus have the same basic structure as the analogous expression for heavy quark production in hadronic collisions. There is, however, an important difference between photon-induced and hadronic collisions, as described, for instance, in [17].

"Here we would like to point out that the way of counting the order of QCD calculations in the photon-induced processes is still a subject of discussion (see, e.g., [21,22] and earlier papers [23,24]). The origin of the problem is the presence of a definite parton model prediction in the form of an $\alpha \ln(Q^2)$ contribution, leading to the inhomogeneous term in the Q^2 evolution equations for the quark densities in the photon. One approach bases on the treatment of the quark density in the photon as being of the order $q^\gamma \sim \alpha/\alpha_s$, while in the second one $q^\gamma \sim \alpha$. This difference leads to different sets of diagrams which formally should be included in the NLO calculations; see, e.g., the prompt photon production at HERA, where two types of NLO predictions are compared to data [25]."

I adhere to the second point of view, as do the authors of [22,23], but contrary to that adopted in [7–9]. As in the

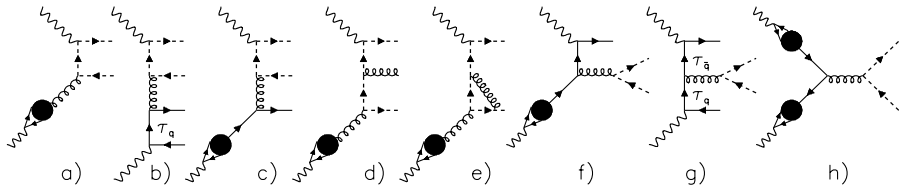

FIG. 2. Examples of resolved photon diagrams involving the pointlike parts of PDF of the photon and the related direct photon diagrams.

case of photoproduction of direct photons, investigated in [22,23], this implies that the set of diagrams which I think should be included in the NLO QCD calculations of $\sigma_{\rm tot}(\gamma\gamma \to b\bar{b})$ does not coincide with that used by the authors of [7–9]. Specifically, I think one should include beside the class A direct photon contribution (which must undoubtedly be included to make the direct photon contribution next-to-leading in α_s) also the classes B and C. I will not elaborate on why I think this is the right way to proceed, as the aim of this paper is to investigate the scale dependence of NLO calculations [7–9] of $\sigma_{\rm tot}(\gamma\gamma \to b\bar{b})$.

III. $\bar{B}B$ PRODUCTION AT LEP2

At LEP the incoming electrons and positrons acted as sources of transverse quasireal photons[1] described by the flux

$$f_T^{\gamma}(y, Q^2) = \frac{\alpha}{2\pi}\left(\frac{1+(1-y)^2}{y}\,\frac{1}{Q^2} - \frac{2m_e^2 y}{Q^4}\right), \qquad (11)$$

where Q^2 stands for photon virtuality. For brevity of notation, we shall in the following write instead of $\sigma_{\rm tot}(e^+e^- \to e^+e^- b\bar{b})$ simply $\sigma_{\rm tot}(e^+e^- \to b\bar{b})$.

Although the data are available only for cross sections integrated over the whole phase space, we shall discuss the contributions $d\sigma_k(e^+e^- \to b\bar{b})/dW$ of individual processes as functions of $\gamma\gamma$ collision energy W. The shapes of these contributions can alternatively be characterized by the functions

$$F_k(W) \equiv \int_{2m_b}^{W} dw\,\frac{d\sigma_k(e^+e^- \to b\bar{b})}{dw}, \qquad G_k(W) \equiv \int_{W}^{\sqrt{S}} dw\,\frac{d\sigma_k(e^+e^- \to b\bar{b})}{dw}, \qquad (12)$$

which quantify how much of a given contribution comes from the region up to a given W [$F_k(W)$] or above it [$G_k(W)$]. As the available data are not copious enough to measure the differential distribution $d\sigma(e^+e^- \to b\bar{b})/dW$, the theoretical analysis of the distributions (12) might allow us to invent a strategy of how to separate the kinematic region of accessible W into two parts, each dominated by a particular contribution. The relative importance of the individual contributions as a function of W is determined by the ratio

$$r_k(W) \equiv \frac{d\sigma_k(e^+e^- \to b\bar{b})}{dW} \Big/ \frac{d\sigma_{\rm tot}(e^+e^- \to b\bar{b})}{dW}. \qquad (13)$$

[1]In the kinematical region relevant for $b\bar{b}$ production in $\gamma\gamma$ collisions at LEP2, the mean photon virtuality was very small, typically $\langle Q^2\rangle \simeq 0.01$ GeV^2, and consequently the contribution of longitudinal virtual photons can be safely neglected.

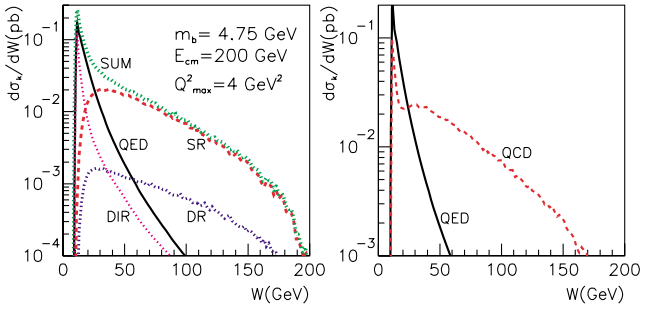

FIG. 3 (color online). Left: The distributions $d\sigma_k/dW$ corresponding to the pure QED contribution together with three lowest order QCD contributions: single resolved (SR), double resolved (DR), and direct (DIR). The sum of all four contributions is shown as the upper dotted curve. Right: The comparison of pure QED contribution with the sum of three lowest order QCD ones. All curves were obtained for $m_b = 4.75$ GeV, $\sqrt{S} = 200$ GeV, and $Q^2_{\rm max} = 4$ GeV^2 using GRV LO PDF of the photon and setting $\Lambda^{(4)} = 0.27$ GeV.

A. QED contribution

The pure QED contribution to $\sigma_{\rm tot}(e^+e^- \to b\bar{b})$ is given as

$$\frac{d\sigma_{\rm QED}(e^+e^- \to b\bar{b})}{dW} = \frac{6\alpha^4 e_b^4}{\pi S}\,\frac{A(W)}{W}\left[\left(1+\frac{4m_b^2}{W^2}-\frac{8m_b^4}{W^4}\right)\times \ln\frac{1+\beta}{1-\beta} - \beta\left(1+\frac{4m_b^2}{W^2}\right)\right], \qquad (14)$$

where

$$A(W) = \iint dy\,dz\,\delta\left(\frac{W^2}{S}-yz\right)\left[\frac{1+(1-y)^2}{y}\right] \times \left[\frac{1+(1-z)^2}{z}\right]\ln\frac{Q^2_{\rm max}(1-y)}{m_e^2 y^2}\,\ln\frac{Q^2_{\rm max}(1-z)}{m_e^2 z^2}, \qquad (15)$$

results from convolution of photon fluxes (11), integrated over the virtualities up to $Q^2_{\rm max}$. The convolution (15) can easily be performed analytically and the result inserted into (14). In Fig. 3, we display by the solid curve the result

TABLE I. The integrated cross sections $\sigma(e^+e^- \to b\bar{b}, S)$ for $\sqrt{S} = 200$ GeV and $Q^2_{\rm max} = 4$ GeV^2, corresponding to the distributions in Fig. 3. The renormalization and factorization scales μ and M we identified and set equal to m_b. LO form of $\alpha_s(\mu)$ was used. All cross sections are in picobarns.

Parameters			QED	LO QCD			Total
m_b	$\Lambda^{(4)}$	PDF		DIR	SR	DR	
4.75	0.27	GRV LO	1.27	0.473	1.415	0.121	3.28
4.5	0.27	GRV LO	1.40	0.478	1.746	0.146	3.77
4.75	0.35	GRV LO	1.27	0.520	1.542	0.141	3.47
4.75	0.27	SAS1D	1.27	0.473	0.904	0.077	2.73

of evaluating (14) for $m_b = 4.75$ GeV, $\sqrt{S} = 200$ GeV, and $Q^2_{\max} = 4$ GeV. The distribution vanishes at the threshold $W = 2m_b$ due to the threshold behavior of the cross section (9), peaks at about $W = 12$ GeV, and then drops rapidly off due to the fast decrease of both the photon flux (11) and (9).

Integrating the distributions in Fig. 3 yields the values in the fourth column of Table I.

B. Lowest order QCD corrections

As in the case of a pure QED contribution (9), these corrections are given as convolutions of the photon flux (11) with the appropriate partonic cross sections. In all calculations, u, d, s, and c quarks were considered as intrinsic in the photon and $n_f = 4$ was correspondingly taken in the expression for $\alpha_s(\mu)$.

The W dependence of the lowest order QCD correction to direct photon contribution is given as the product

$$\frac{d\sigma^{\rm LO}_{\rm dir}(W)}{dW} = \frac{6\alpha^4 e_b^4}{\pi S}\frac{A(W)}{W}\alpha_s(\mu)\sigma^{(1)}_{\rm dir}(W/m_b). \qquad (16)$$

The resulting W dependence evaluated for $\mu = m_b$ and shown in Fig. 3 is peaked even more sharply at small W than the pure QED contribution (14). This reflects the fact that the cross section $\sigma^{(1)}_{\rm dir}(W/m_b)$ does not vanish at the threshold $W = 2m_b$ as does $\sigma^{(0)}_{\rm dir}(W/m_b)$.

The lowest order single and double resolved photon contributions were computed with HERWIG Monte Carlo event generator, which implements the appropriate LO cross sections of the processes

$$\gamma + G \to b + \bar{b}, \qquad (17)$$

$$G + G \to b + \bar{b}, \qquad q + \bar{q} \to b + \bar{b}, \qquad (18)$$

where $q = u, d, s, c$ stand for intrinsic quarks in the photon, and convolutes them with photon fluxes and PDF of the quasireal photon(s). In HERWIG, the renormalization and factorization scales μ and M are identified and set equal to an expression which is approximately equal to the transverse mass $\mu = M = M_T \equiv \sqrt{E_T^2 + m_b^2}$. In the LEP2 energy range, the mean $\langle M_T \rangle$ depends weakly on W with, approximately, $\langle M_T \rangle \simeq 7$ GeV.

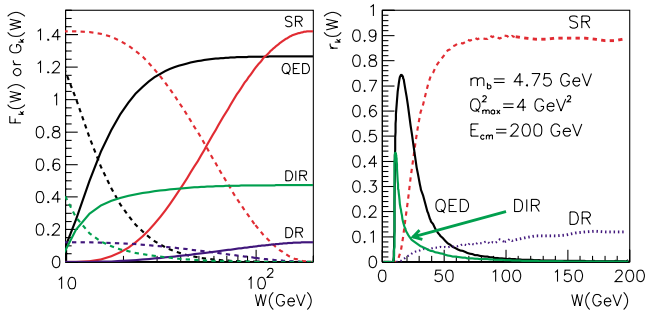

FIG. 4 (color online). Left: Solid (dashed) curves show the partially integrated cross sections $F_k(W)$ ($G_k(W)$) defined in (12) for QED and three lowest order QCD contributions. Right: The relative contributions $r_k(W)$ defined in (13) for the same four contributions.

Results of the calculations, in which the LO GRV PDF of the photon, the LO expression for $\alpha_s(\mu)$ with $\Lambda^{(4)} = 0.27$ GeV, and $m_b = 4.75$ GeV were used, are shown in Figs. 3 and 4. As expected, the corresponding distributions are much broader than those of pure QED or lowest order QCD direct contributions.

C. Comparison of individual contributions

The comparison of the distributions $d\sigma_k/dW$, $F_k(W)$, $G_k(W)$, and $r_k(W)$, corresponding to four individual contributions, displayed in Figs. 3 and 4, and summarized in Table I, reveals a large difference in their shapes and magnitude. Specifically, we conclude that

(i) The pure QED as well as the lowest order QCD direct photon contributions peak at very small W and are basically negligible above $W \simeq 50$ GeV. For instance, the left plot of Fig. 4 shows that 95% of the QED contribution comes from the region $W \lesssim 30$ GeV.

(ii) The onset of single and double resolved photon contributions are much slower, but these distributions are, on the other hand, markedly broader.

(iii) The double resolved photon contribution is practically negligible everywhere.

(iv) The pure QED and single resolved photon contributions are of comparable size and together make up about 85% of the total integrated cross section,

(v) up to about $W \simeq 30$ GeV, $d\sigma_{\rm tot}/dW$ is dominated by pure QED contribution, whereas for $W \gtrsim 30$ GeV QCD contributions take over.

The numbers given in Table I correspond to standard fractionally charged quarks. In [26], its author interprets the excess of data over standard theoretical calculations as evidence for Hahn-Nambu integer quark charges. I think his argumentation is wrong, but I mention it here to illustrate the merit of separating the data into at least two regions of W. Were the author of [26] right, the whole discrepancy would have come from the region of small W, where QED contribution dominates.

On the other hand, were the light gluino production [15] responsible for the observed excess, this excess would have to come from the region of W dominated by the double resolved photon contribution. Although the energy dependence of the gluon-gluon fusion to gluino-antigluino may be slightly different than those of $G + G \to Q\bar{Q}$ or $q\bar{q} \to Q\bar{Q}$, the basic shape of the W distributions is given by the convolution of the photon fluxes (11) and the gluon distribution function of the photon, which are the same in both types of processes.

The above observations underline the fact that, in order to pin down the origins of the excess of the integrated cross section $\sigma_{\rm tot}(e^+e^- \to b\bar{b})$ over theoretical calculations, it would be helpful to have the data separated into at least two subsamples, say $W \lesssim 30$ GeV and $W \gtrsim 30$ GeV.

The magnitude of the contributions discussed in the preceding subsection depend, beside the renormalization and factorization scales specified above, on a number of other input parameters: the numerical values of m_b, $\Lambda^{(4)}_{\rm QCD}$, $Q^2_{\rm max}$. The calculations reported above were performed for $\sqrt{S} = 200$ GeV, $Q^2_{\rm max} = 4$ GeV^2, $m_b = 4.75$ GeV, and $\Lambda^{(4)} = 0.27$ GeV using the GRV LO PDF of the photon. To see the sensitivity of the LO results to these assumptions we varied some of these parameters:

(i) m_b was lowered to $m_b = 4.5$ GeV,
(ii) $\Lambda^{(4)}$ was increased to 0.35 GeV,
(iii) GRV set of PDF of the photon was replaced with that of Schuler-Sjöstrand set SAS1D.

The choice of $Q^2_{\rm max} = 4$ GeV^2 corresponds roughly to the usual cuts imposed on the LEP2 data and could therefore be also adjusted to specific conditions of a given experiment. The results of the calculations of $\sigma_{\rm tot}(e^+e^- \to e^+e^- b\bar{b})$, corresponding to different sets of input parameters specified above, are listed in Table I. Lowering m_b increases all four contributions, as does, except for the pure QED one, increasing $\Lambda^{(4)}$. SAS1D PDF yield markedly lower results for single and double resolved photon contributions. It is, however, clear that varying the input parameters within reasonable bounds does not bring the sum of lowest order QED and QCD calculations significantly closer to the data.

IV. CAN HIGHER ORDER QCD CORRECTIONS SOLVE THE PUZZLE?

With the sum of QED and lowest order QCD contributions way below the data, we shall now address the question of how much of this gap can be explained by the higher order QCD corrections.

A. Direct photon contribution

As emphasized above, in order to obtain an expression of the next-to-leading order in α_s, the direct photon term of the order $\alpha_s^2 \sigma^{(2)}_{\rm dir}$ must be added to the lowest order QCD contribution (10). Because the latter is proportional to e_b^4, the class A of $\alpha^2\alpha_s^2$ direct photon contributions is needed for this purpose. The sum of the second and third terms in (1), i.e., dropping the purely QED contribution, can be written as

$$\sigma^{\rm NLO}_{\rm dir}(W, m_b, \mu) \equiv \sigma^{(1)}_{\rm dir}(W, m_b)\alpha_s(\mu) \times [1 + r_1(W, m_b, \mu)\alpha_s(\mu)]. \quad (19)$$

The NLO coefficient r_1 has the general form

$$r_1(W, m_b, \mu, {\rm RS}) = \frac{\beta_0}{4\pi} \ln\frac{\mu^2}{\Lambda^2_{\rm RS}} - \rho(W/m_b), \quad (20)$$

where $\rho(W, m_b)$ denotes the renormalization scale and scheme invariant [16], which governs the basic features of the scale dependence of (19):

$\rho > 0$: The expression (19), considered as a function of μ, exhibits a stationary point (local maximum) where it is locally stable. This point, preferred by the principle of minimal sensitivity [16], is also close to the point for which $r_1 = 0$, which is selected by the method of effective charges [27]. The value of $\sigma^{\rm NLO}_{\rm dir}$ at the stationary point is proportional to $1/\rho$ implying large NLO corrections for small ρ. Inserting the appropriate numbers for $n_f = 4$, $m_b = 4.75$ GeV, and $\Lambda^{(4)}_{\overline{\rm MS}} = 0.27$ GeV, we get

$$\rho(W/m_b) = 3.88 - r_1(W/m_b, 1, \overline{\rm MS}). \quad (21)$$

The coefficient $r_1(W/m_b, 1, \overline{\rm MS})$ thus does not have to be too large to get small, or even negative ρ.

$\rho \le 0$: $\sigma^{\rm NLO}_{\rm dir}$ is a monotonous function of μ, in fact even steeper than $\sigma^{\rm LO}_{\rm dir}$. Consequently, for negative ρ going to the NLO does not improve the stability of the calculation, but quite on the contrary.

As the second term in (19) has not yet been calculated, we cannot associate the class A direct photon contribution, given by the first term in (19), to a well-defined renormalization scheme. Moreover, as the magnitude of the NLO corrections in (19) is determined by the ratio $\sigma^{(2)}_{\rm dir}(W/m_b, 1)/\sigma^{(1)}_{\rm dir}(W/m_b)$ of two functions of W/m_b, which may depend on W/m_b in different ways, the coefficient r_1 may be very large even when both the numerator and denominator are on average of comparable and small magnitude. This indicates that, without the knowledge of class A direct photon contribution of the order $\alpha^2\alpha_s^2$, we cannot make a meaningful estimate of the importance of the second term in (19).

B. Resolved photon contribution

As for LEP2 energies, the double resolved photon one is numerically negligible, only the single resolved photon contribution will be discussed in detail below. As shown in Fig. 3, $d\sigma^{\rm LO}_{\rm sr}/dW$ peaks at about $W = 30$ GeV with the mean value $\langle W \rangle \doteq 65$ GeV. This suggests that the cross section $\sigma^{\rm NLO}_{\rm sr}(e^+e^- \to b\bar{b})$ will be determined primarily by those of $\sigma^{\rm NLO}_{\rm sr}(\gamma\gamma \to b\bar{b})$ in the energy range $30 \lesssim W \lesssim 65$ GeV.

All the results shown below for the single resolved photon contribution,

$$\sigma_{\rm sr}^{\rm NLO}(W, M, \mu) = 2\alpha_s(\mu) \int dx\, G(x, M)[\sigma_{\gamma G}^{(1)}(x) + \alpha_s(\mu)\sigma_{\gamma G}^{(2)}(x, M, \mu)] + 4\alpha_s^2(\mu) \times \int dx \sum_i q_i(x, M)\sigma_{\gamma q_i}^{(2)}(x, M), \tag{22}$$

are based on the formulas for the partonic cross sections $\sigma_{ij}^{(k)}$ as given in [28] and were obtained using the GRV HO set of PDF of the photon and setting $\Lambda_{\overline{\rm MS}}^{(4)} = 0.27$. Because the expressions for $\sigma_{\gamma G}^{(2)}$ as given in [28] correspond to $\mu = M$, we have reconstituted its separate dependence on μ and M by adding to $\sigma_{\gamma G}^{(2)}(x, M, M)$ the term $(\beta_0/4\pi)\sigma_{\gamma G}^{(1)} \ln(\mu^2/M^2)$. Note that for each value of M the expression (22) has, as far as the μ dependence is concerned, the form of the NLO expression (19).

We first follow the conventional procedure and set $M = \mu$. The resulting scale dependence of the expression (22), together with those of the quark and gluon contributions to it, are shown in Fig. 5(a) for $W = 40$ GeV. Overlaid for comparison is also the LO approximation, given by the first term in (22). We note the different scale dependence of the γG and γq channels, the latter turning negative for $M \gtrsim 6$ GeV, but the most important observation concerns the fact that the conventional NLO approximation (22) is a monotonously decreasing function of the scale $M = \mu$. Moreover, it falls off even steeper than the LO expression. In other words, in going from the leading to the next-to-leading order in α_s the sensitivity to the scale variation increases, rather than decreases, as one might expect (and hope).

Recalling the discussion in Sec. IVA, one should, however, not be surprised. To check how much this feature depends on setting exactly $\mu = M$, we plot in Fig. 5(b)

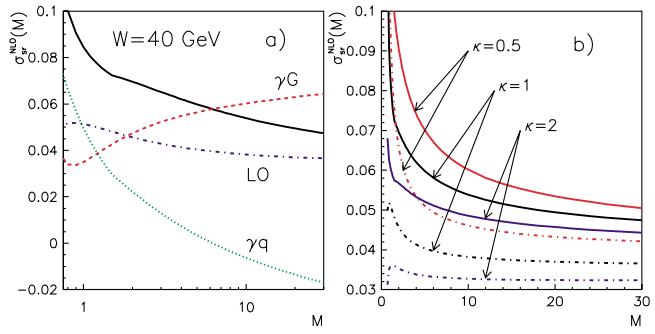

FIG. 5 (color online). (a) The scale dependence of the conventional NLO approximation $\sigma_{\rm sr}^{\rm NLO}(W, M, M)$ for $W = 40$ GeV (solid curve) together with the contributions of the γG (dashed) and $\gamma q/\bar{q}$ (dotted) channels. The LO approximation is shown for comparison by the dash-dotted curve. (b) $\sigma_{\rm sr}^{\rm NLO}(W, M, \kappa M)$ (solid curve) and $\sigma_{\rm sr}^{\rm LO}(W, M, \kappa M)$ (dash-dotted) for $W = 40$ GeV and three values of $\kappa = 0.5, 1.2$.

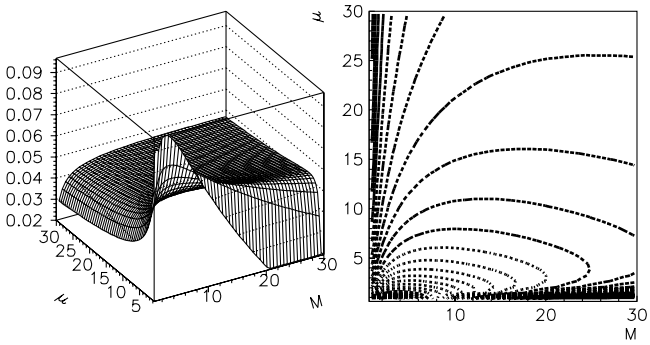

FIG. 6. The surface and contour plots of $\sigma_{\rm sr}^{\rm NLO}(W, M, \mu)$ for $W = 40$ GeV.

the scale dependence of $\sigma_{\rm sr}^{\rm NLO}(W, M, \mu = \kappa M)$ for standard choices of $\kappa = 0.5, 1, 2$. Clearly, the above conclusion is independent of κ in this range.

The steep and monotonous scale dependence of $\sigma_{\rm sr}^{\rm NLO}(W, M, \mu = \kappa M)$ is a clear warning that the conventional NLO approximation is unstable. To see what happens if we relax the usual but arbitrary identification $\mu = \kappa M$, we plot in Fig. 6 the surface and contour plots representing the full M and μ dependence of $\sigma_{\rm sr}^{\rm NLO}(W, M, \mu)$ as given in Eq. (22).

Contrary to the analogous process in antiproton-proton collisions [12], it does not exhibit a saddle point, where the derivatives with respect to both M and μ would vanish, but Fig. 6 seems to indicate some sort of stability region at large scales, say for $M \gtrsim 10$ GeV, $\mu \gtrsim 20$ GeV. This impression is, however, misleading as becomes clear if we plot in Fig. 7 the slices of the surface plot in Fig. 6 along both axes and recall the discussion of Sec. IVA. For each fixed value of the factorization scale M, the expression (22) has a form of the NLO expression as far as the

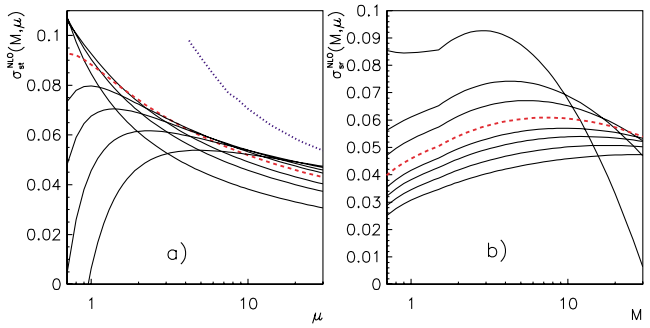

FIG. 7 (color online). The renormalization scale dependence of $\sigma_{\rm sr}^{\rm NLO}(W, M, \mu)$ for fixed values of the factorization scale (a) and vice versa: The factorization scale dependence of $\sigma_{\rm sr}^{\rm NLO}(W, M, \mu)$ for the same set of fixed values of the renormalization scale μ (b). All calculations correspond to $W = 40$ GeV. In (a) the ordering from above of the curves at $\mu = 30$ GeV corresponds to $M = 30, 16, 10, 7, 4.75, 3, 2$, and 1 GeV. In (b) the curves correspond at $M = 0.7$ GeV to the same sequence from below.

renormalization scale μ is concerned. Recalling the discussion in Sec. IVA, we see that for $M \lesssim 4.2$ GeV $\sigma_{\rm sr}^{\rm NLO}(M, \mu)$ corresponds to negative ρ and thus exhibits no local stability point. For higher M the local maximum in the μ dependence of $\sigma_{\rm sr}^{\rm NLO}(M, \mu)$ exists at the associated $\mu_{\rm max}(M)$. The M dependence of $\sigma_{\rm sr}^{\rm NLO}[M, \mu_{\rm max}(M)]$, shown in Fig. 7(a) by the dotted curve, is, however, even steeper than those at fixed M. The above plots and conclusions concerned the results at one typical value of W, but their essence holds for the whole interval relevant for LEP2 data.

We thus conclude that in the energy range relevant for LEP2 data the renormalization and factorization scale dependence of the conventional NLO calculations of single resolved photon contribution to the total cross section $\sigma_{\rm tot}(\gamma\gamma \to b\bar{b})$ exhibit no stability region, either as a function of the common scale $\mu = \kappa M$ or as a fully two dimensional function of μ and M.

V. SUMMARY AND CONCLUSIONS

We have seen that in order to understand the origin of the discrepancy between LEP2 data on $b\bar{b}$ production in $\gamma\gamma$ collisions and the currently available theoretical calculations the separation of data into at least two bins of the hadronic energy W, say $W \lesssim 30$ GeV and $W \gtrsim 30$ GeV, could be instrumental in pinning down the possible mechanisms or phenomena responsible for the observed excess.

We have also shown that the existing NLO QCD calculations are very sensitive to the variation of renormalization and factorization scale, exhibiting no region of local stability. This indicates that the results based on the standard choice of renormalization and factorization scales $\mu = M = m_b$ should be taken with great caution. It is clear that the class A direct photon term of the order $\alpha^2\alpha_s^2$ is needed to make the direct photon contribution of next-to-leading order in α_s. My conjecture is that order $\alpha^2\alpha_s^2$ direct photon terms of class B and C, which are related to single and double resolved photon contributions, may help stabilize the latter with respect to the variation of renormalization and factorization scales.

ACKNOWLEDGMENTS

The work has been supported by the Ministry of Education of the Czech Republic under Project No. LN00A006. The conversations with N. Arteaga, M. Cacciari, C. Carimalo, F. Kapusta, and W. Da Silva are gratefully acknowledged.

[1] D0 Collaboration, B. Abbott *et al.*, Phys. Rev. Lett. **85**, 5068 (2000).
[2] CDF Collaboration, D. Acosta *et al.*, Phys. Rev. D **65**, 052005 (2002).
[3] H1 Collaboration, C. Adloff *et al.*, Phys. Lett. B **467**, 156 (1999); **518**, 331(E) (2001).
[4] ZEUS Collaboration, J. Breitweg *et al.*, Eur. Phys. J. C **18**, 625 (2001).
[5] L3 Collaboration, M. Acciarri *et al.*, Phys. Lett. B **503**, 10 (2001).
[6] OPAL Collaboration, A. Csilling, AIP Conf. Proc. **571**, 276 (2000).
[7] M. Drees, M. Krämer, J. Zunft, and P. Zerwas, Phys. Lett. B **306**, 371 (1993).
[8] M. Krämer and E. Laenen, Phys. Lett. B **371**, 303 (1996).
[9] S. Frixione, M. Krämer, and E. Laenen, Nucl. Phys. **B571**, 169 (2000).
[10] ZEUS Collaboration, S. Chekanov *et al.*, hep-ex/0405069.
[11] M. Cacciari and P. Nason, Phys. Rev. Lett. **89**, 122003 (2002).
[12] J. Chýla, J. High Energy Phys. **03** (2003) 042.
[13] DELPHI Collaboration, W. Da Silva *et al.*, Nucl. Phys., Sect. B Proc. Suppl. **126**, 185 (2004).
[14] H. Jung, Phys. Rev. D **65**, 034015 (2002).
[15] E. Berger *et al.*, Phys. Rev. Lett. **86**, 4231 (2001).
[16] P. M. Stevenson, Phys. Rev. D **23**, 2916 (1981).
[17] M. Krawczyk, A. Zembrzuski, and M. Staszel, Phys. Rep. **345**, 265 (2001).
[18] H. D. Politzer, Nucl. Phys. **B194**, 493 (1984).
[19] J. Chýla, hep-ph/0111469.
[20] J. H. Kühn, E. Mirkes, and J. Steegborn, Z. Phys. C **57**, 615 (1993).
[21] J. Chýla, J. High Energy Phys. **04** (2000) 007.
[22] M. Krawczyk and A. Zembrzuski, *Proceedings of ICHEP'98, Vancouver, Canada, 1998* (World Scientific, Singapore, 1999), p. 895
[23] M. Krawczyk, Acta Phys. Pol. B **21**, 999 (1990).
[24] A. C. Bawa, M. Krawczyk, and W. J. Stirling, Z. Phys. C **50**, 293 (1991).
[25] ZEUS Collaboration, J. Breitweg *et al.*, Phys. Lett. B **472**, 175 (2000).
[26] P. Ferreira, hep-ph/0209156.
[27] G. Grunberg, Phys. Rev. D **29**, 2315 (1984).
[28] R. K. Ellis and P. Nason, Nucl. Phys. **B312**, 551 (1989).